

## **Online Supplemental Material (Parekh et al.)**

Aron Parekh,<sup>†</sup> Nazanin S. Ruppender,<sup>§</sup> Kevin M. Branch,<sup>†</sup> M. K. Sewell-Loftin,<sup>¶</sup> Jun Lin,<sup>§</sup> Patrick D. Boyer,<sup>§</sup> Joseph E. Candiello,<sup>||</sup> W. David Merryman,<sup>¶</sup> Scott A. Guelcher,<sup>§</sup> and Alissa M. Weaver<sup>†‡\*</sup>

<sup>†</sup>Department of Cancer Biology and <sup>‡</sup>Department of Pathology, University Medical Center, Nashville, Tennessee;  
<sup>§</sup>Department of Chemical and Biomolecular Engineering, and <sup>¶</sup>Department of Biomedical Engineering, Vanderbilt University, Nashville, Tennessee; and <sup>||</sup>Department of Bioengineering, University of Pittsburgh, Pittsburgh, Pennsylvania

## **Supplemental Methods**

### **Swelling**

The swelling ratio was calculated as follows:

$$Q = v_2^{-1} = \rho_p \left[ \left( \frac{Q_m}{\rho_s} \right) + \left( \frac{1}{\rho_p} \right) \right]$$

where  $v_2^{-1}$  is the volume fraction,  $\rho_p$  is the protein density assumed to be 1.27 g/cm<sup>3</sup> for collagen,  $\rho_s$  is the water density assumed to be 1 g/cm<sup>3</sup>, and  $Q_m$  is the mass ratio of water to protein. Protein fractions were calculated as the inverse of the swelling ratio (i.e., volume fraction of protein).

### **AFM of UBM-BM stromal and BM surfaces**

The modulus, E, is calculated by the software with the following equation (1):

$$F_{\text{tip}} = \frac{4}{3} E \sqrt{Rd^3} + F_{\text{adh}}$$

$F_{\text{tip}}$  is the force on the tip, E is the Young's modulus, R is the tip radius, d is the distance between the sample and the tip, and  $F_{\text{adh}}$  is the adhesive force between the tip and the sample. Raw moduli values were plotted versus percentage of total area within a sample. Scan parameters were: scan size 5  $\mu\text{m}$  x 5  $\mu\text{m}$ , peak force set point 1 nN, and maximum modulus 25 MPa. The AFM probe tips were silicon-nitride cantilever (SNL) from Veeco, with spring constants between 0.07 – 0.1 N/m and radii between 25 – 40 nm. Each tip was calibrated for spring constant and radius prior to sample measurements. Tissue samples were hydrated in PBS and held taut during AFM scans in Cell Crown inserts, with the system inverted so that the tissue was not resting on the bottom of the Petri dish during the scans. For modulus determination, three independent samples of tissue were scanned and the weighted average of the modulus for each area scanned was calculated as follows:

$$E = \frac{\sum w_i E_i}{\sum w_i}$$

where  $w_i$  is the percent of times a modulus of value  $E_i$  was observed. Adjacent sections of each sample were taken, so that measurements could be made of both stroma and BM sides of each sample. A total of three measurements per sample per side were taken.

### **Quantitative real-time PCR**

To measure changes in gene expression, mRNA reverse transcription was carried out using the SuperScript III kit (Invitrogen) per manufacturer's instructions. Briefly, total RNA was extracted using the RNeasy Mini Kit (Qiagen). The SuperScript III First Strand Synthesis System for quantitative RT-PCR primed with random hexamers was used to synthesize cDNA using between 1 and 5 $\mu$ g total RNA. In order to obtain enough RNA, invadopodia assays on the different synthetic substrates were scaled up and performed in either 60 mm Petri dish lids or 12-well plates for the PAAs and PURs, respectively, and seeded with ~15,000-50,000 cells/cm<sup>2</sup>. The expression of ADAMTS1, MMP1, LAMB1, and MMP14 was measured by quantitative RT-PCR using validated TaqMan primers with the 7300 Real-Time PCR System (Applied Biosystems). Assays were performed in triplicate on the RealPlex Machine (Eppendorf) under the following cycling conditions following a 10-minute incubation period at 95°C: 95°C for 15 seconds, 60°C for 60 seconds. The expression of OPN was determined using SYBR green primers as described previously (2). Quantification was performed using the  $\Delta\Delta$ ct method using 18S as an internal control.

### Supplemental Figure and Table Legends

**Supplemental Figure 1. Quantitation of invadopodia activity in 804G cells cultured on synthetic invadopodia substrates.** (A) Similar to the results with CA1d cells, degradation area per cell peaked statistically on the hard PAA substrates (i.e., significantly different from the soft PAA and glass). (B) Number of total invadopodia (actively degrading and non-degrading) per cell peaked statistically on both the hard PAA (10 kPa) and the glass (69 GPa) (i.e., significantly different from the soft PAA but not each other). (C) Number of actively degrading invadopodia per cell (as identified by colocalization of actin and cortactin over black degraded areas only) were not statistically different although values were small since 804G cells do not make as many invadopodia/cell as CA1d cells. (D) Cell sizes on the soft PAA and glass were statistically significant from each other but neither were significantly different from the hard PAA value. Data were highly nonparametric and therefore presented as box and whisker plots with the solid lines indicating the medians, whiskers representing the 95% confidence intervals, and dots representing outliers. For comparisons depicted on the graphs, \* indicates  $p < 0.05$  as described above for specific comparisons.  $n = 143, 126,$  and  $170$  cells for the soft PAA, hard PAA, and glass substrates, respectively combined from 3 independent experiments.

**Supplemental Figure 2. Gene expression in MCF10A CA1d breast carcinoma cells is regulated across a wide rigidity range.** Relative fold changes in mRNA levels of ADAMTS1 (ADAM metalloproteinase with thrombospondin type 1 motif, 1) peaked on the more compliant PAAs ( $E = 1-30$  kPa) while MMP1 (matrix metalloproteinase 1) levels peaked on the more rigid T900 PUR ( $E = 6$  MPa). Significant differences were also found in expression levels between some of the PURs ( $E = 6$  MPa-2GPa) and PAAs ( $E = 1-30$  kPa) for OPN (osteopontin) and LAMB1 (laminin, beta1) as well indicating the ability of these cells to respond to different orders of magnitude in rigidity. No differences were found in the expression of MMP14 (matrix metalloproteinase 14) on any of the substrates. Data were normalized to 18S expression and shown as fold changes compared to the Soft PAA. Data are presented as mean  $\pm$  standard error, and \* and \*\* indicates  $p < 0.05$  for pairwise and group comparisons, respectively. Gene expression was measured in triplicate for each experiment and overall for 3 independent experiments on the 4 substrates.

**Supplemental Figure 3. Quantitation of invadopodia numbers in 804G cells plated on stromal and BM sides of UBM-BM.** Invadopodia (arrows) were identified by colocalization of actin (red) and cortactin (blue) for quantification on the (A) stroma and (B) BM using confocal and widefield fluorescence imaging, respectively. (C) Quantitation of invadopodia formation by 804G bladder carcinoma cells reveals a statistically significant increase ( $p < 0.05$ ) in the total invadopodia per cell (based number of actin- and cortactin-double positive puncta) in cells cultured on the stromal side of UBM-BM, as compared to the BM

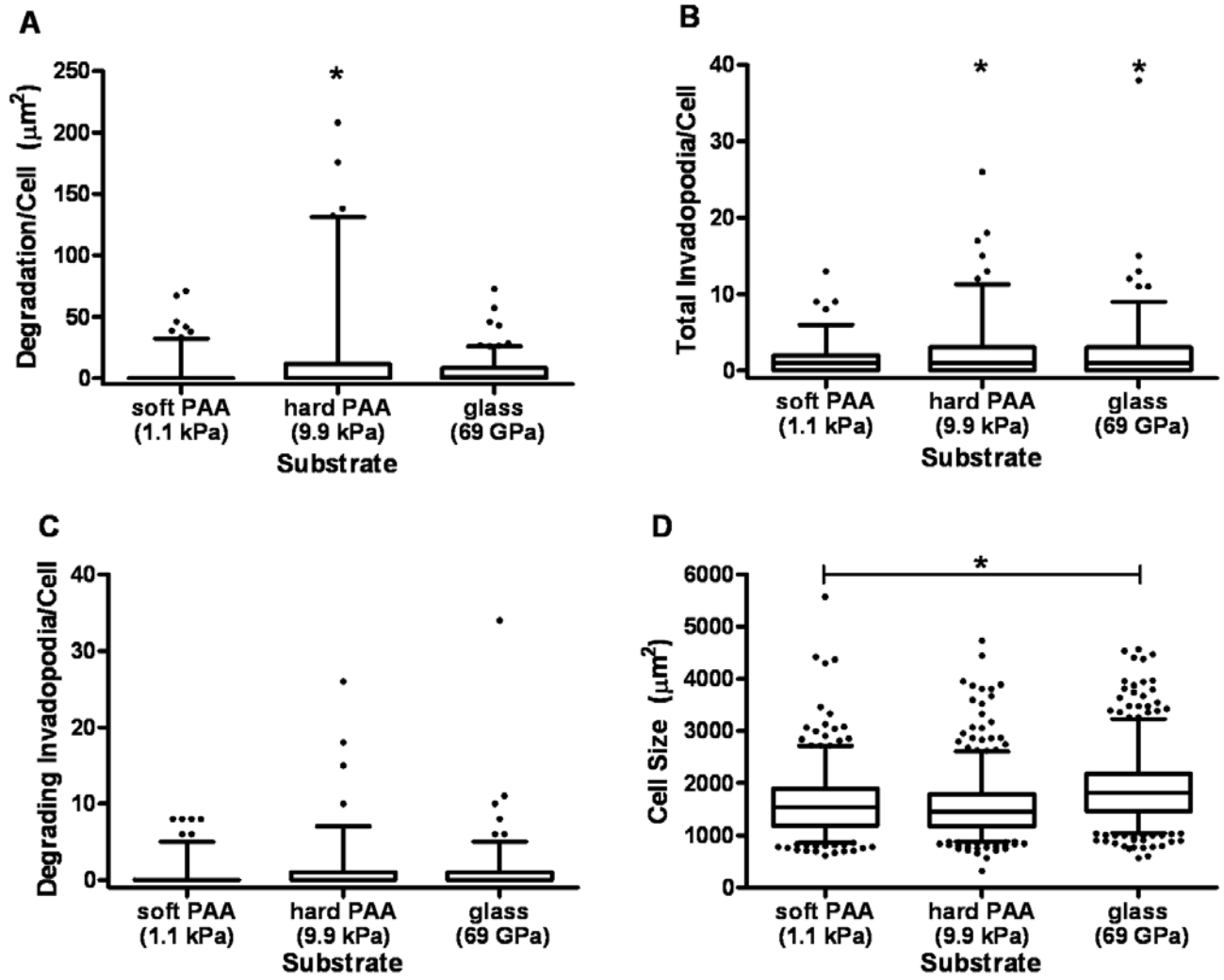
side. Data were highly nonparametric and are presented as an area fill, and n=171 and 163 cells for the stromal and BM sides, respectively, from 2 independent experiments.

**Supplemental Table 1. All statistical comparisons for Figure 6 with \* indicating  $p < 0.05$ .** Results of statistical analyses as described in the Materials and Methods section for MCF10A CA1d breast carcinoma cancer cell invadopodia activity on the different substrates for (A) degradation area per cell, (B) number of total invadopodia per cell, (C) number of invadopodia actively degrading ECM per cell, and (D) cell size.

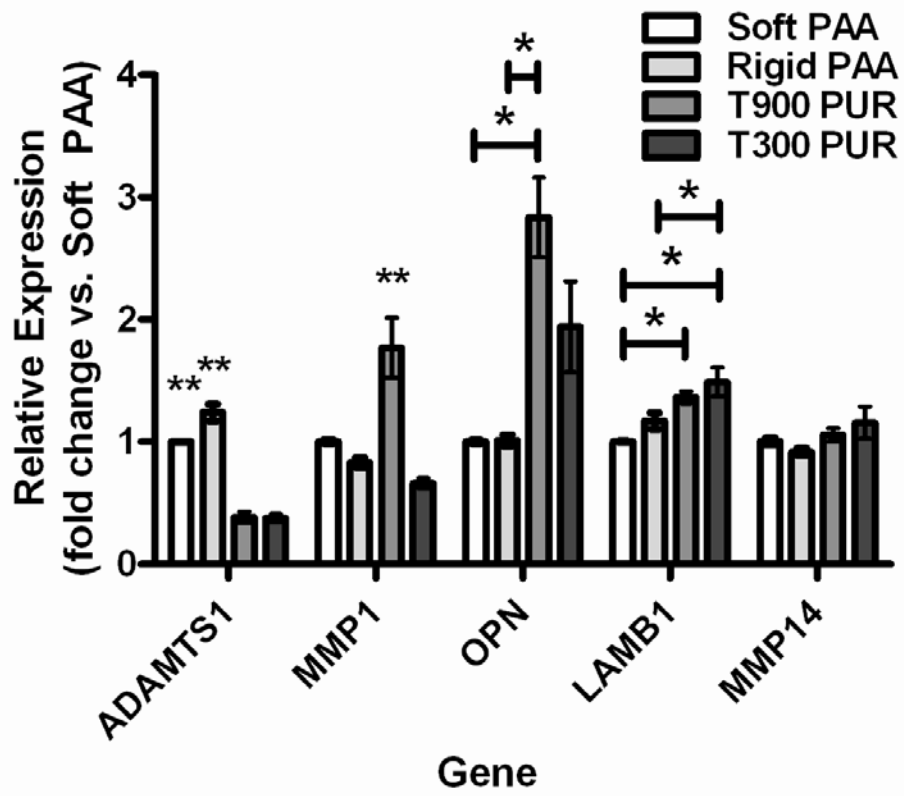
### Supplemental References

1. Derjaguin, B. V., V. M. Muller, and Y. P. Toropov. 1975. Effect of contact deformations on the adhesion of particles. *J Colloid Interface Sci* 53:314-326.
2. Javelaud, D., K. S. Mohammad, C. R. McKenna, P. Fournier, F. Luciani, M. Niewolna, J. Andre, V. Delmas, L. Larue, T. A. Guise, and A. Mauviel. 2007. Stable overexpression of Smad7 in human melanoma cells impairs bone metastasis. *Cancer Res* 67:2317-2324.

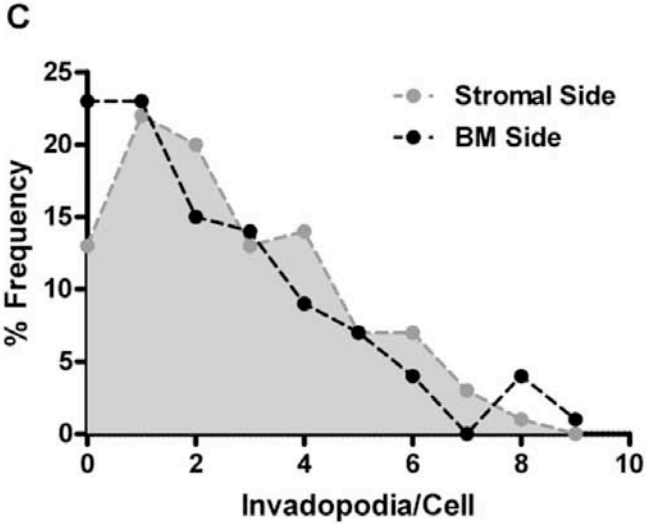
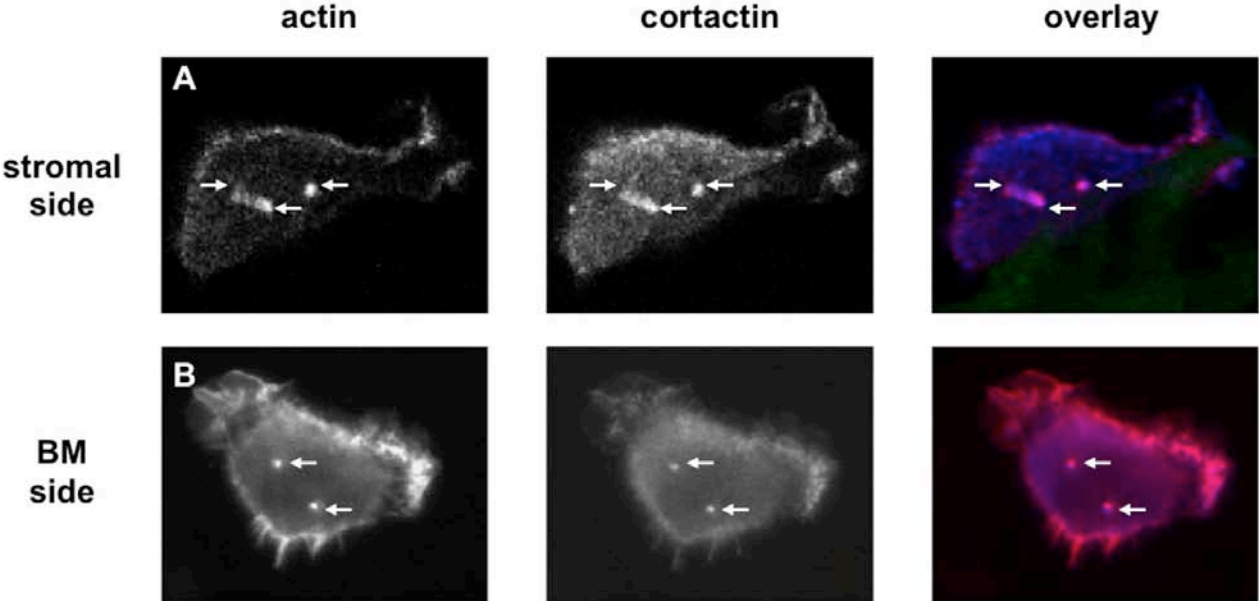
Supplemental Figure 1



Supplemental Figure 2



Supplemental Figure 3



Supplemental Table 1

(A)	soft PAA	hard PAA	rigid PAA	T3000 PUR	T900 PUR	T300 PUR	glass
soft PAA	N/A	*	*	*	*	*	*
hard PAA	*	N/A	*		*	*	
rigid PAA	*	*	N/A	*	*	*	*
T3000 PUR	*		*	N/A	*		
T900 PUR	*	*	*	*	N/A		*
T300 PUR	*	*	*			N/A	*
glass	*		*		*	*	N/A

(B)	soft PAA	hard PAA	rigid PAA	T3000 PUR	T900 PUR	T300 PUR	glass
soft PAA	N/A	*	*	*		*	*
hard PAA	*	N/A	*		*	*	
rigid PAA	*	*	N/A	*	*		*
T3000 PUR	*		*	N/A		*	
T900 PUR		*	*		N/A	*	*
T300 PUR	*	*		*	*	N/A	
glass	*		*		*		N/A

(C)	soft PAA	hard PAA	rigid PAA	T3000 PUR	T900 PUR	T300 PUR	glass
soft PAA	N/A	*	*	*	*	*	*
hard PAA	*	N/A	*				
rigid PAA	*	*	N/A	*	*	*	*
T3000 PUR	*		*	N/A	*		
T900 PUR	*		*	*	N/A	*	
T300 PUR	*		*		*	N/A	
glass	*		*				N/A

(D)	soft PAA	hard PAA	rigid PAA	T3000 PUR	T900 PUR	T300 PUR	glass
soft PAA	N/A				*		*
hard PAA		N/A			*	*	*
rigid PAA			N/A				*
T3000 PUR				N/A	*		*
T900 PUR	*	*		*	N/A		
T300 PUR		*				N/A	*
glass	*	*	*	*		*	N/A